Inverse Problems and Imaging
Volume 7, No. 4, 2013, X–XX
doi:10.3934/ipi.2013.7.xx

FACTORIZATION METHOD FOR THE INVERSE STOKES PROBLEM

Armin Lechleiter and Tobias Rienmüller

Zentrum für Technomathematik
Universität Bremen
28359 Bremen, Germany

(Communicated by Andreas Kirsch)

Abstract. We propose an imaging technique for the detection of porous inclusions in a stationary flow based on the Factorization method. The stationary flow is described by the Stokes-Brinkmann equations, a standard model for a flow through a (partially) porous medium, involving the deformation tensor of the flow and the permeability tensor of the porous inclusion. On the boundary of the domain we prescribe Robin boundary conditions that provide the freedom to model, e.g., in- or outlets for the flow. The direct Stokes-Brinkmann problem to find a velocity field and a pressure for given boundary data is a mixed variational problem lacking coercivity due to the indefinite pressure part. It is well-known that indefinite problems are difficult to tackle theoretically using Factorization methods. Interestingly, the Factorization method can nevertheless be applied to this non-coercive problem, as long as one uses data consisting only of velocity measurements. We provide numerical experiments showing the feasibility of the proposed technique.

1. **Introduction.** The inverse problem that we consider in this paper is to image penetrable inclusions modeled by the Stokes-Brinkmann equations in a bounded Lipschitz domain $\Omega \subset \mathbb{R}^d$, $d = 2$ or 3, with Robin boundary conditions. These equations describe a fluid in steady-state in terms of the velocity field $u = (u_1, \dots, u_d)^\top : \Omega \to \mathbb{R}^d$ and the pressure $p : \Omega \to \mathbb{R}$. Both quantities are related through the deformation tensor $D(u)$ of the fluid,

$$D(u) := \frac{1}{2}\left(\nabla u + (\nabla u)^\top\right), \qquad \text{where } \nabla u = \begin{pmatrix} \frac{\partial u_1}{\partial x_1} & \cdots & \frac{\partial u_1}{\partial x_d} \\ \vdots & \ddots & \vdots \\ \frac{\partial u_d}{\partial x_1} & \cdots & \frac{\partial u_d}{\partial x_d} \end{pmatrix}$$

and where $A^\top$ denotes the transposed matrix of a matrix $A \in \mathbb{R}^{n\times m}$. The Stokes-Brinkmann equations

$$-\operatorname{div}(\mu D(u)) + Mu + \nabla p = f \qquad \text{in } \Omega \tag{1}$$

further involve the (scalar) viscosity $\mu : \Omega \to \mathbb{R}$ of the fluid and the matrix-valued function $M : \Omega \to \mathbb{R}^{d\times d}$. The latter function corresponds, roughly speaking, to the inverse of the permeability tensor (scaled by the viscosity) of porous inclusions inside the domain Ω. The latter equation is complemented by the divergence constraint

$$\operatorname{div} u = 0 \qquad \text{in } \Omega. \tag{2}$$

2010 *Mathematics Subject Classification.* Primary: 35R30, 65N21; Secondary: 76D07.
Key words and phrases. Inverse boundary value problem, Stokes equation, factorization method.

We should mention already at this point that our notation does not respect some of the usual notational conventions in the physics literature for viscous flows. Most differences are intended to reduce the number of required symbols and allow for a compact notation.

The Stokes-Brinkmann equations are particularly important, at various scales, for modeling flow through porous and partially porous media. Possible applications include for instance the modeling of flow of liquids or gas through the ground, see, e.g., [18, 23] that investigate flow through carbonate karst reservoirs in detail. The problem of detecting inclusions in flows could moreover be applied to non-destructive testing problems of isolation materials by streaming air into a block of the material and measuring the resulting outflow.

On the boundary $\Gamma := \partial\Omega$ we prescribe Robin boundary conditions for the normal and tangential components of the velocity field. These conditions go back to Navier, see [22]; they will be introduced in (8) below. These conditions offer considerably more flexibility to model boundary phenomena than pure Dirichlet (or *no-slip*) or Neumann boundary conditions. The Robin conditions for instance allow to crudely model outlets on the boundary of the domain where liquid or gas streams in or out. However, since these boundary conditions necessarily link the pressure, the deformation tensor, and the velocity field, it is impossible to eliminate the pressure in (1) by, e.g., seeking merely for a velocity field in spaces of divergence-free functions (the latter technique would be applicable, e.g., when considering no-slip boundary conditions).

The explicit appearance of the pressure in the boundary conditions complicates the analysis of the direct and the inverse problem. First, the variational problem for the direct Stokes-Brinkmann problem necessarily yields a mixed, non-coercive variational formulation that is coercive in the velocity variable but indefinite in the pressure variable. Of course, this mixed formulation can be tackled using standard inf-sup conditions. Second, it is well-known that the analysis of the Factorization method requires, roughly speaking, coercivity of the direct problem. In our framework, the indefiniteness of the direct problem does not perturb the analysis of the Factorization method for the inverse problem, as long as one considers (difference) measurements that are merely based on the velocity field. The analysis that we present would indeed not work for any (reasonable) measurements involving pressure.

The number of publications on inverse problems for Stokes(-Brinkmann) equations and related partial differential equations is relatively small when compared to, e.g., the Laplace, the Helmholtz, or the Maxwell's equations, and most papers appeared quite recently. Among the work that is most related to ours is a paper on a point source method for the Oseen equation (a linearization of the Navier-Stokes equations), see [26], and a Factorization method for the Stokes equations, see [25], as well as non-linear integral equations for reconstructing obstacles in a Stokes flow, see [2]. In contrast to our paper, these works consider flows in an unbounded domain for impenetrable obstacles with no-slip (Dirichlet) boundary conditions for the velocity field. Usually, the viscosity μ outside the obstacle is constant, and the term $\operatorname{div}(\mu D(u))$ becomes a multiple of the (vectorial) Laplacian. For such problems one can avoid to solve an indefinite problem involving the velocity field and the pressure, for example by solving an integral equation of the second kind for a single unknown density.

Other algorithmic techniques for solving inverse problems involving stationary flows include shape optimization techniques [5] for the shape reconstruction of impenetrable cavities, and topological derivatives for the localization of small cavities [3]. For identifiability and stability results for the linear Stokes equations (and partially also for the time-independent, non-linear Navier-Stokes equation), see [1, 4, 14]. Finally, [7] even considers inverse (obstacle) problems for time-dependent flows.

Let us finally comment on a technical detail due to the divergence constraint in (2). All velocities appearing in this paper are divergence-free functions. Together with the divergence theorem this implies that the two Robin-to-Dirichlet operators $\Lambda_{0,1}$ for the direct Stokes(-Brinkmann) equations with and without inclusion vanish when they are applied to a constant multiple of the outside unit normal vector n to Ω. In principle, one could hence factor out this one-dimensional kernel. We decided not to do so, since the mixed variational formulation for the velocity-pressure pair is nevertheless uniquely solvable for any (bounded, linear) right-hand side. In some sense, the above-described kernel re-appears when we consider the relative Robin-to-Dirichlet operator $\Lambda_0 - \Lambda_1$, see Theorem 3.7 for details.

We close this introduction by a couple of less important technical remarks: All results of this paper remain correct if the porous inclusions possesses the same viscosity as the background medium. However, the permeability tensor *must* have contrast for the proof of Theorem 4.1; stated in our notation, the proof of this theorem requires that $y^\top M(x)y > c|y|^2$ for points x in the inclusion D and $0 \neq y \in \mathbb{R}^d$. Interestingly, this issue is merely linked with the construction of a divergence-free sampling function for the Factorization method, but not with the range identity. All of our results also hold if $y^\top M(x)y > 0$ for $x \in D$ and $0 \neq y \in \mathbb{R}^d$, at least if the inverse "square root" $M^{-1/2}$ does not explode too fast at the boundary of Ω, compare [16]. Such weaker assumptions, however, require somewhat more involved proofs. A couple of interesting and practically relevant problems that we do not treat in this paper are for instance the detection of inclusions on the boundary of the domain, or the detection of changes in the boundary coefficients.

This paper is organized as follows: We introduce the Stokes and Stokes-Brinkmann equations together with their variational formulations in Section 2. The inverse problem of identifying the shape of a penetrable inclusion from boundary measurements in introduced in Section 3, followed by an analysis of the factorization of the measurement operator. Section 4 recalls the well-known fundamental solution and the Green's function of the Stokes equations. Section 5 contains the main characterization result of the paper, and Section 6 presents an (academic) numerical example that illustrates feasibility, advantages and disadvantages of the method. The appendix collects a couple of well-known auxiliary results, including, e.g., several variants of Korn's inequality we rely on.

Notation. We denote by $H^1(\Omega)^d = \{u \in L^2(\Omega)^d,\, \partial u_i/\partial x_j \in L^2(\Omega) \text{ for } i,j = 1,\dots,d\}$ the standard first-order L^2-based Sobolev space equipped with usual first-order Sobolev norm. In the entire text $\Omega \subset \mathbb{R}^d$, where $d = 2$ or 3, is a Lipschitz domain. The boundary of Ω is Γ and n is the unit outward-pointing normal vector to Ω. We define an inner product for matrices by $A{:}B := \sum_{i,j=1}^d A_{ij}B_{ij}$ for $A, B \in \mathbb{R}^{d\times d}$; the associated norm is $|A| = \sqrt{A{:}A}$. The corresponding inner product on $L^2(\Omega)^{d\times d} := L^2(\Omega, \mathbb{R}^{d\times d})$ is

$$\langle A, B\rangle_{L^2(\Omega)^{d\times d}} := \int_\Omega A(x){:}B(x)\,\mathrm{d}x \qquad \text{for } A, B \in L^2(\Omega)^{d\times d}.$$

2. **Stokes flow and variational formulation.** The Stokes equations describe incompressible viscous fluids at low Reynolds number in the steady state. The governing equations for the velocity $u:\ \Omega \to \mathbb{R}^d$ and the pressure $p:\ \Omega \to \mathbb{R}$ are

$$\begin{aligned} -\mathrm{div}\,(\mu D(u)) + \nabla p &= f \qquad \text{in } \Omega, \\ \mathrm{div}\, u &= 0 \qquad \text{in } \Omega, \end{aligned} \tag{3}$$

with suitable boundary conditions of Robin type that we introduce below. The coefficient $\mu:\ \Omega \to \mathbb{R}$ denotes the fluid's viscosity and $f:\ \Omega \to \mathbb{R}^d$ is a source term. The second equation in (3) is the so-called incompressibility condition for the fluid. In contrast to many papers and textbooks on the Stokes equations, we do not assume here that the viscosity μ is constant. Note that a direct computation shows that for constant viscosity, the term $\mathrm{div}\,(\mu D(u))$ reduces (in the distributional sense) to $\mu\Delta u\,/2$, where the Laplacian is applied component-wise.

Lemma 2.1. *If $u \in H^1(\Omega)^d$ such that $\mathrm{div}\, u = 0$, then $\Delta u = 2\,\mathrm{div}\, D(u)$.*

All differential equations in this text will be formulated variationally. To this end, the next lemma provides an essential integration-by-parts formula.

Lemma 2.2. *For $\mu \in L^\infty(\Omega)$ and $u \in H^1(\Omega)^d$ such that $\mathrm{div}\,(\mu D(u)) \in L^2(\Omega)$ it holds that*

$$-\int_\Omega v^\top \mathrm{div}\,(\mu D(u))\,\mathrm{d}x = \int_\Omega \mu D(v){:}D(u)\,\mathrm{d}x - \int_\Gamma v^\top (\mu D(u) n)\,d\sigma \qquad \forall v \in H^1(\Omega)^d. \tag{4}$$

The right-most term has to be interpreted as a duality product of $v^\top \in H^{1/2}(\Gamma)^d$ with the co-normal derivative $\mu D(u)n \in H^{-1/2}(\Gamma)^d$, see [21]. Seeking for a solution $u \in H^1(\Omega)^d$ to (3) we multiply the first equation with a test function $v \in H^1(\Omega)^d$, integrate over Ω, and apply Lemma 2.2 as well as the divergence theorem,

$$\begin{aligned} \int_\Omega D(v){:}\mu D(u)\,\mathrm{d}x \;-\; \int_\Omega p\,\mathrm{div}\, v\,\mathrm{d}x \;+\; \int_\Gamma v^\top (pn - \mu D(u)n)\,\mathrm{d}S \\ = \int_\Omega v^\top f\,\mathrm{d}x \quad \forall v \in H^1(\Omega)^d. \end{aligned} \tag{5}$$

Let us now consider the boundary terms in (5). Every vector field u on the boundary can be decomposed into its tangential component $v_\parallel$ and its normal component $v_\perp$,

$$v = v_\parallel + v_\perp = \begin{cases} n \times (v \times n) + (v \cdot n)\, n, & d = 3, \\ (v_1 n_2 - v_2 n_1) \left(\begin{smallmatrix} n_2 \\ -n_1 \end{smallmatrix}\right) + (v_1 n_1 + v_2 n_2) \left(\begin{smallmatrix} n_1 \\ n_2 \end{smallmatrix}\right), & d = 2. \end{cases} \tag{6}$$

The same decomposition can be done for the vector field $D(u)n$,

$$D(u)\,n = D_\parallel(u) + D_\perp(u) = \begin{cases} n \times ((D(u)n) \times n) + ((D(u)n) \cdot n)\, n, & d = 3, \\ \left[(D(u)\,n \cdot \left(\begin{smallmatrix} n_2 \\ -n_1 \end{smallmatrix}\right)\right] \left(\begin{smallmatrix} n_2 \\ -n_1 \end{smallmatrix}\right) \\ \qquad + \left[D(u)\,n \cdot \left(\begin{smallmatrix} n_1 \\ n_2 \end{smallmatrix}\right)\right] \left(\begin{smallmatrix} n_1 \\ n_2 \end{smallmatrix}\right), & d = 2. \end{cases}$$

Hence, $v^\top (D(u)\,n) = [v_\parallel + v_\perp]^\top [D_\parallel(u) + D_\perp(u)] = v_\parallel^\top\, D_\parallel(u) + v_\perp^\top\, D_\perp(u)$ and (5) becomes

$$\begin{aligned} \int_\Omega \mu D(u){:}D(v)\,\mathrm{d}x \;-\; \int_\Omega p\,\mathrm{div}\, v\,\mathrm{d}x \;-\; \int_\Gamma v_\parallel^\top (\mu D_\parallel(u))\,\mathrm{d}S \\ + \int_\Gamma v_\perp^\top (pn - \mu D_\perp(u))\,\mathrm{d}S \;=\; \int_\Omega v^\top f\,\mathrm{d}x\,. \end{aligned} \tag{7}$$

Remark 1. Strictly speaking, we would have to restrict a vector field $u \in H^1(\Omega)^d$ to the boundary Γ before taking its normal or tangential component. To simplify notation, we will nevertheless write $u_\perp$ and $u_\parallel$ instead of $(u|_\Gamma)_\perp$ and $(u|_\Gamma)_\parallel$ for $u \in H^1(\Omega)^d$, respectively.

We want the tangential and normal components of u and of the deformation tensor $D(u)$ to satisfy Robin-type boundary conditions,

$$\mu D_\parallel(u) = g_\parallel - \alpha_\parallel u_\parallel \text{ on } \Gamma \quad \text{and} \quad pn - \mu D_\perp(u) = -g_\perp + \alpha_\perp u_\perp \text{ on } \Gamma \tag{8}$$

for given boundary data $g \in L^2(\Gamma)^d$. Plugging these relations into (7) yields that

$$\begin{aligned} \int_\Omega \mu D(u){:}D(v)\,\mathrm{d}x + \int_\Gamma \alpha_\parallel v_\parallel^\top u_\parallel\,\mathrm{d}S + \int_\Gamma \alpha_\perp v_\perp^\top u_\perp\,\mathrm{d}S - \int_\Omega p\,\mathrm{div}\,v\,\mathrm{d}x \\ = \int_\Omega v^\top f\,\mathrm{d}x + \int_\Gamma v_\parallel^\top g_\parallel\,\mathrm{d}S + \int_\Gamma v_\perp^\top g_\perp\,\mathrm{d}S \qquad \forall v \in H^1(\Omega)^d. \end{aligned} \tag{9}$$

For given $f \in L^2(\Omega)^d$ and $g \in L^2(\Gamma)^d$, the variational formulation to find $u \in H^1(\Omega)^d$ and $p \in L^2(\Omega)$ will be presented below, under the assumption that $\mu \in L^\infty(\Omega)$ and $\alpha_{\perp,\parallel} \in L^\infty(\Gamma)$ are positive. Before stating this mixed formulation, let us introduce the Stokes-Brinkmann equations.

A penetrable porous inclusion inside the viscous liquid can be modeled by the Stokes-Brinkmann equations: Using the above notation, these equations describe the steady-state flow via an additional absorption term $M : \Omega \to \mathbb{R}^{d\times d}$ that is typically supported inside the inclusions,

$$\begin{aligned} -\mathrm{div}(\mu D(u)) + Mu + \nabla p &= f && \text{in } \Omega, \\ \mathrm{div}\,u &= 0 && \text{in } \Omega, \\ \mu D_\parallel(u) + \alpha_\parallel u_\parallel &= g_\parallel && \text{on } \Gamma, \\ (\mu D_\perp(u) - pn) + \alpha_\perp u_\perp &= g_\perp && \text{on } \Gamma. \end{aligned} \tag{10}$$

The material parameters μ and M will typically take different values in the inside and the outside of a porous inclusion. In particular, outside the inclusion the flow is free, that is, M vanishes.

To state existence and uniqueness results for the Stokes(-Brinkmann) equations, we suppose that $\mu \in L^\infty(\Omega)$ is strictly positive, $\mu \geq c > 0$, that $\alpha_{\perp,\parallel} \in L^\infty(\Gamma)$ with $\alpha_{\perp,\parallel} \geq c > 0$, and that $M \in L^\infty(\Omega)^{d\times d}$ takes values in the symmetric and positive semidefinite matrices,

$$y^\top M(x) y \geq 0 \qquad \forall x \in \Omega \text{ and } y \in \mathbb{R}^d.$$

Define the bounded bilinear forms

$$a(u,v) := \int_\Omega \mu D(u){:}D(v)\,\mathrm{d}x + \int_\Omega v^\top Mu\,\mathrm{d}x + \int_\Gamma \alpha_\parallel v_\parallel^\top u_\parallel\,\mathrm{d}S + \int_\Gamma \alpha_\perp v_\perp^\top u_\perp\,\mathrm{d}S\,, \tag{11}$$

$$b(v,p) := -\int_\Omega p\,\mathrm{div}\,v\,\mathrm{d}x\,, \qquad \text{and } F(v) := \int_\Omega v^\top f\,\mathrm{d}x + \int_\Gamma v^\top g\,\mathrm{d}S \tag{12}$$

for $u, v \in H^1(\Omega)^d$, $p \in L^2(\Omega)$, $f \in L^2(\Omega)^d$ and $g \in L^2(\Gamma)^d$. Repeating exactly the same integrations by parts that lead us to (9) we obtain the following mixed variational formulation of the Stokes-Brinkmann equations (10), which obviously

include the Stokes equations by setting $M = 0$: Seek $u \in H^1(\Omega)^d$ and $p \in L^2(\Omega)$ such that

$$a(u,v) + b(v,p) = F(v) \qquad \forall v \in H^1(\Omega)^d, \tag{13}$$

$$b(u,q) = 0 \qquad \forall q \in L^2(\Omega). \tag{14}$$

Theorem 2.3. *For any bounded linear form $F : H^1(\Omega)^d \to \mathbb{R}$ there exists a unique solution $(u,p) \in H^1(\Omega)^d \times L^2(\Omega)$ of the variational problem (13).*

Proof. This is an application of a standard result on mixed variational formulations, see [6]. For the problem under investigation, one uses Korn's inequality (see Lemma A.2(b)) to show coercivity of the bilinear form $a(\cdot,\cdot)$, and an inf-sup condition for the form b, see, e.g., [20, 6]. □

Remark 2. Different physically senseful choices for the boundary conditions on Γ are possible, e.g., $u_\parallel = 0$ and $(\mu D_\perp(u) - pn) + \alpha_\perp u_\perp = g_\perp$ on Γ. The ansatz space for the solution u is then $H^1_\perp(\Omega)^d = \{u \in H^1(\Omega)^d : u_\parallel = 0 \text{ on } \Gamma\}$. The formulation (7) has to be adapted by replacing $H^1(\Omega)^d$ by $H^1_\perp(\Omega)^d$ and skipping the term involving $\alpha_\parallel$. It is also possible to replace *all* Robin boundary conditions by Neumann conditions. Then, however, the solution space has to be adapted, typically yielding a quotient space where rigid motions are factored out.

3. **Inverse Stokes problem and factorization of the data operator.** In this section we consider an inverse Stokes problem which is to reconstruct an inclusion $D \subset \Omega$ where both viscosity and permeability differ from the background parameters from boundary measurements taken on $\Gamma = \partial\Omega$. To this end, we denote by μ_0 the *known* viscosity of the background medium, while μ_1 denotes the unknown viscosity which differs from μ_0 inside an unknown inclusion $D \subset \Omega$. In the entire paper we assume that $\Omega\backslash\bar{D}$ is connected. We also assume that the viscosity inside the inclusion is higher than in the background medium, and that the permeability inside D is positive. As above, we describe the permeability effect by a symmetric matrix $M : \Omega \to \mathbb{R}^{d\times d}$ such that $M(x) = 0$ a.e. in $\Omega\backslash\bar{D}$ and $y^\top M(x) y \geq c|y|^2 > 0$ for a.e. $x \in D$ and all $0 \neq y \in \mathbb{R}^d$. In the following, we abbreviate this property as

$$M \geq c > 0.$$

Later on, it will be convenient to work with the viscosity contrast κ,

$$\kappa := \begin{cases} \mu_1 - \mu_0 & \text{for } x \in D, \\ 0 & \text{for } x \in \Omega\backslash\bar{D}. \end{cases}$$

The reconstruction of the shape of D is based on the difference of two Robin-to-Dirichlet operators. Roughly speaking, the first of these operators, $\Lambda_0 : L^2(\Gamma)^d \to L^2(\Gamma)^d$, maps Robin boundary values to the trace of the solution u_0 to the Stokes problem with (background) viscosity μ_0 (and without the Brinkmann term M). The second of these operators, $\Lambda_1 : L^2(\Gamma)^d \to L^2(\Gamma)^d$, does the same for viscosity μ_1 and permeability M. More precisely, Λ_0 maps $g \in L^2(\Gamma)^d$ to $u_0|_\Gamma$, where $(u_0, p_0) \in H^1(\Omega)^d \times L^2(\Omega)$ solves

$$\begin{aligned} \int_\Omega \mu_0 D(u_0){:}D(v)\,\mathrm{d}x \;+\; \int_\Gamma \alpha_\parallel v_\parallel^\top (u_0)_\parallel \,\mathrm{d}S \;+\; \int_\Gamma \alpha_\perp v_\perp^\top (u_0)_\perp \,\mathrm{d}S \;-\; \int_\Omega p_0 \operatorname{div} v \,\mathrm{d}x \\ +\; \int_\Omega q \operatorname{div} u_0 \,\mathrm{d}x \;=\; \int_\Gamma v^\top g \,\mathrm{d}S \qquad \forall v \in H^1(\Omega)^d, \forall q \in L^2(\Omega). \end{aligned} \tag{15}$$

Remark 3. (a) In (15) we added the incompressibility condition from the second line of (13) to the first line of (13). Of course, choosing $v = 0$ in (15) shows that this condition is still satisfied.

(b) The operator Λ_0 can in principle be computed (numerically) without knowing D, M, or μ_1; it is hence not necessarily required to measure Λ_0 experimentally. If, however, such measurements are available, then the modeling error of the difference $\Lambda_0 - \Lambda_1$ can be reduced significantly.

Analogously, the Robin-to-Dirichlet operator Λ_1 maps g to $u_1|_\Gamma$, where the pair $(u_1, p_1) \in H^1(\Omega)^d \times L^2(\Omega)$ solves

(16)
$$\int_\Omega \mu_1 D(u_1){:}D(v)\,\mathrm{d}x + \int_D v^\top M u_1\,\mathrm{d}x + \int_\Gamma \alpha_\parallel v_\parallel^\top (u_1)_\parallel\,\mathrm{d}S + \int_\Gamma \alpha_\perp v_\perp^\top (u_1)_\perp\,\mathrm{d}S - \int_\Omega p_1 \operatorname{div} v\,\mathrm{d}x + \int_\Omega q \operatorname{div} u_1\,\mathrm{d}x = \int_\Gamma v^\top g\,\mathrm{d}S \quad \forall v \in H^1(\Omega)^d,\ \forall q \in L^2(\Omega).$$

Theorems 2.3 and A.1 show that $\Lambda_{0,1}$ are well-defined and compact operators on $L^2(\Gamma)^d$.

A crucial tool to arrive at a Factorization method for the inverse Stokes-Brinkmann problem is a factorization of the relative Robin-to-Dirichlet operator $\Lambda_0 - \Lambda_1$. To construct this factorization we set $\Lambda_0 g = u_0|_\Gamma$ and $\Lambda_1 g = u_1|_\Gamma$ and write $w = u_0 - u_1$ and $r = p_0 - p_1$. We take the difference of (15) and (16), use the fact that $\mu_0 = \mu_1 - \kappa$, and find that

(17)
$$\int_\Omega \mu_1 D(w){:}D(v)\,\mathrm{d}x + \int_D v^\top M w\,\mathrm{d}x + \int_\Gamma \alpha_\parallel v_\parallel^\top w_\parallel\,\mathrm{d}S + \int_\Gamma \alpha_\perp v_\perp^\top w_\perp\,\mathrm{d}S - \int_\Omega r \operatorname{div} v\,\mathrm{d}x + \int_\Omega q \operatorname{div} w\,\mathrm{d}x = \int_D \kappa D(u_0){:}D(v)\,\mathrm{d}x + \int_D v^\top M u_0\,\mathrm{d}x \quad \forall v \in H^1(\Omega)^d,\ \forall q \in L^2(\Omega).$$

To derive a first factorization of $\Lambda_0 - \Lambda_1$ we define the (evaluation) operator $H : L^2(\Gamma)^d \to H^1(D)^d$ to evaluate the field u_0 for background viscosity μ_0 in the inclusion D,

$$H : g \mapsto u_0|_D\,,$$

where $(u_0, p_0) \in H^1(\Omega)^d \times L^2(\Omega)$ solves (15). Additionally, we define the solution operator

$$G : H^1(D)^d \to L^2(\Gamma)^d \quad \text{by} \quad Gh = w,$$

where $(w, r) \in H^1(\Omega)^d \times L^2(\Omega)$ solves

(18)
$$\int_\Omega \mu_1 D(w){:}D(v)\,\mathrm{d}x + \int_D v^\top M w\,\mathrm{d}x + \int_\Gamma \alpha_\parallel v_\parallel^\top w_\parallel\,\mathrm{d}S + \int_\Gamma \alpha_\perp v_\perp^\top w_\perp\,\mathrm{d}S - \int_\Omega r \operatorname{div} v\,\mathrm{d}x + \int_\Omega q \operatorname{div} w\,\mathrm{d}x = \int_D \kappa D(h){:}D(v)\,\mathrm{d}x + \int_D v^\top M h\,\mathrm{d}x \quad \forall v \in H^1(\Omega)^d,\ \forall q \in L^2(\Omega).$$

Comparing the last mixed variational formulation with (17) directly shows the factorization $\Lambda_0 - \Lambda_1 = GH$. In the following we will need to work with the adjoint H^* of H. We compute this adjoint with respect to the (special) inner product

(19)
$$\langle h_1, h_2 \rangle_* = \int_D \kappa D(h_1){:}D(h_2)\,\mathrm{d}x + \int_D h_2^\top M h_1\,\mathrm{d}x\,.$$

Lemma 3.1. *If $\kappa \geq c > 0$ and if $y^\top M(x) y \geq c|y|^2 > 0$ a.e. in D and for all $0 \neq y \in \mathbb{R}^d$, then the inner product from (19) is equivalent to the usual inner product on $H^1(D)^d$.*

Proof. The proof follows from the coercivity of the bilinear form in (19) due to Lemma A.2(a). □

Theorem 3.2. *The adjoint $H^* : H^1(D)^d \to L^2(\Gamma)^d$ is given by $H^* h = v|_\Gamma$ where $v \in H^1(\Omega)^d$ and $s \in L^2(\Omega)$ solve*

$$\begin{aligned}(20)\quad &\int_\Omega \mu_0 D(v){:}D(\psi)\,\mathrm{d}x + \int_\Gamma \alpha_\parallel \psi_\parallel^\top v_\parallel \,\mathrm{d}S + \int_\Gamma \alpha_\perp \psi_\perp^\top v_\perp \,\mathrm{d}S - \int_\Omega s\,\mathrm{div}\,\psi\,\mathrm{d}x \\ &+ \int_\Omega q\,\mathrm{div}\,v\,\mathrm{d}x = \int_D \kappa D(h){:}D(\psi)\,\mathrm{d}x + \int_D \psi^\top M h\,\mathrm{d}x \\ &\qquad\qquad \forall \psi \in H^1(\Omega)^d,\ \forall q \in L^2(\Omega).\end{aligned}$$

Proof. Let $h \in H^1(D)^d$ and $g \in L^2(\Gamma)^d$. By definition of the inner product (19) and by definition of H,

$$\begin{aligned}\langle h, Hg\rangle_* &= \int_D \kappa D(h){:}D(Hg)\,\mathrm{d}x + \int_D (Hg)^\top M h\,\mathrm{d}x \\ &= \int_D \kappa D(h){:}D(u_0)\,\mathrm{d}x + \int_D u_0^\top M h\,\mathrm{d}x\,,\end{aligned}$$

where $(u_0, p_0) \in H^1(\Omega)^d \times L^2(\Omega)$ solves (15). Next, we use (20) with $(\psi, q) = (u_0, p_0)$ to get that

$$\begin{aligned}\int_D \kappa D(h){:}D(u_0)\,\mathrm{d}x + \int_D u_0^\top M h\,\mathrm{d}x &= \int_\Omega \mu_0 D(u_0){:}D(v)\,\mathrm{d}x + \int_\Gamma \alpha_\parallel v_\parallel^\top (u_0)_\parallel \,\mathrm{d}S \\ &+ \int_\Gamma \alpha_\perp v_\perp^\top (u_0)_\perp \,\mathrm{d}S - \int_\Omega s\,\mathrm{div}\,u_0\,\mathrm{d}x + \int_\Omega p_0\,\mathrm{div}\,v\,\mathrm{d}x \overset{(15)}{=} \int_\Gamma v^\top g\,\mathrm{d}S\,.\end{aligned}$$

Hence, $\langle h, Hg\rangle_* = \int_\Gamma v^\top g\,\mathrm{d}S$, meaning that $H^* h = v|_\Gamma$ where $(v, s) \in H^1(\Omega)^d \times L^2(\Omega)$ solves (20). □

Theorem 3.3. *The operator $H^* : H^1(D)^d \to L^2(\Gamma)^d$ is compact.*

Proof. This follows from the trace theorem, see Theorem A.1. □

Theorem 3.4. *The factorization*

$$(21)\qquad \Lambda_0 - \Lambda_1 = H^* T H$$

holds with $T : H^1(D)^d \to H^1(D)^d$ defined by $Th = h - w$ where $(w, r) \in H^1(\Omega)^d \times L^2(\Omega)$ solves

$$\begin{aligned}(22)\quad &\int_\Omega \mu_1 D(w){:}D(v)\,\mathrm{d}x + \int_D v^\top M w\,\mathrm{d}x + \int_\Gamma \alpha_\parallel v_\parallel^\top w_\parallel \,\mathrm{d}S + \int_\Gamma \alpha_\perp v_\perp^\top w_\perp \,\mathrm{d}S \\ &- \int_\Omega r\,\mathrm{div}\,v\,\mathrm{d}x + \int_\Omega q\,\mathrm{div}\,w\,\mathrm{d}x = \int_D \kappa D(h){:}D(v)\,\mathrm{d}x + \int_D v^\top M h\,\mathrm{d}x \\ &\qquad\qquad \forall v \in H^1(\Omega)^d,\ \forall q \in L^2(\Omega).\end{aligned}$$

Proof. We exploit that $\mu_1 = \mu_0 + \kappa$ to rewrite the variational formulation (18) that defines $G(h) = w|_\Gamma$ by taking all integrals containing κ or M on the right-hand side,

$$\begin{aligned}(23)\quad &\int_\Omega \mu_0 D(w){:}D(v)\,\mathrm{d}x + \int_\Gamma \alpha_\parallel v_\parallel^\top w_\parallel\,\mathrm{d}S + \int_\Gamma \alpha_\perp v_\perp^\top w_\perp\,\mathrm{d}S - \int_\Omega r\,\mathrm{div} v\,\mathrm{d}x \\ &\quad + \int_\Omega q\,\mathrm{div} w\,\mathrm{d}x = \int_D \kappa D(h-w){:}D(v)\,\mathrm{d}x + \int_D v^\top M(h-w)\,\mathrm{d}x \\ &\qquad\qquad \forall v \in H^1(\Omega)^d,\ \forall q \in L^2(\Omega).\end{aligned}$$

Since we already know that $\Lambda_0 - \Lambda_1 = GH$, it remains to use the definition of H^* in (20) to show that $H^*T = G$ to conclude that (21) holds true. Hence, we need to show that $H^*(h-w) = w|_\Gamma$. If $H^*(h-w) = \widetilde{w}|_\Gamma$ then $(\widetilde{w}, \widetilde{s}) \in H^1(\Omega)^d \times L^2(\Omega)$ solves

$$\begin{aligned}(24)\quad &\int_\Omega \mu_0 D(\widetilde{w}){:}D(\psi)\,\mathrm{d}x + \int_\Gamma \alpha_\parallel \psi_\parallel^\top \widetilde{w}_\parallel\,\mathrm{d}S + \int_\Gamma \alpha_\perp \psi_\perp^\top \widetilde{w}_\perp\,\mathrm{d}S - \int_\Omega \widetilde{s}\,\mathrm{div}\psi\,\mathrm{d}x \\ &\quad + \int_\Omega q\,\mathrm{div}\widetilde{w}\,\mathrm{d}x = \int_D \kappa D(h-w){:}D(\psi)\,\mathrm{d}x + \int_D \psi^\top M(h-w)\,\mathrm{d}x \\ &\qquad\qquad \forall \psi \in H^1(\Omega)^d,\ \forall q \in L^2(\Omega).\end{aligned}$$

Obviously, (24) is exactly the same variational problem for the unknowns $(\widetilde{w}, \widetilde{s})$ as (23) for (w, s). Since this problem is uniquely solvable (see Theorem 2.3) we conclude that $w = \widetilde{w}$. In consequence, $H^*(Th) = H^*(h-w) = \widetilde{w}|_\Gamma = w|_\Gamma = G(h)$. □

Theorem 3.5. *The operator $T : H^1(D)^d \to H^1(D)^d$, $h \mapsto h - w$, where $(w, r) \in H^1(\Omega)^d \times L^2(\Omega)$ solves (22), is self-adjoint on $(H^1(D), \langle\cdot,\cdot\rangle_*)$; see (19) for a definition of the inner product $\langle\cdot,\cdot\rangle_*$.*

Proof. For $h_{1,2} \in H^1(\Omega)^d$ let $(w_{1,2}, r_{1,2}) \in H^1(\Omega)^d \times L^2(\Omega)$ be the solution to (22). We need to show that

$$\begin{aligned}\langle Th_1,\, h_2\rangle_* &= \int_D \kappa D(h_1 - w_1){:}D(h_2)\,\mathrm{d}x + \int_D h_2^\top M(h_1 - w_1)\,\mathrm{d}x \\ &\overset{!}{=} \int_D \kappa D(h_1){:}D(h_2 - w_2)\,\mathrm{d}x + \int_D (h_2 - w_2)^\top M h_1\,\mathrm{d}x = \langle h_1,\, Th_2\rangle_*.\end{aligned}$$

Subtracting $\int_D \kappa D(h_1){:}D(h_2)\,\mathrm{d}x + \int_D h_2^\top M h_1\,\mathrm{d}x$ on both sides, it remains to show that

$$(25)\quad \int_D \left(\kappa D(w_1){:}D(h_2) + h_2^\top M w_1\right)\,\mathrm{d}x \overset{!}{=} \int_D \left(\kappa D(h_1){:}D(w_2) + w_2^\top M h_1\right)\,\mathrm{d}x\,.$$

The variational formulation (22) for (w_2, r_2) with (w_1, r_1) as test functions shows that the left-hand side of (25) equals

$$\begin{aligned}&\int_\Omega \mu_1 D(w_2){:}D(w_1)\,\mathrm{d}x + \int_D w_1^\top M w_2\,\mathrm{d}x + \int_\Gamma \alpha_\parallel (w_1)_\parallel^\top (w_2)_\parallel\,\mathrm{d}S \\ &\qquad + \int_\Gamma \alpha_\perp (w_1)_\perp^\top (w_2)_\perp\,\mathrm{d}S - \int_\Omega r_2\,\mathrm{div} w_1\,\mathrm{d}x - \int_\Omega r_1\,\mathrm{div} w_2\,\mathrm{d}x\,.\end{aligned}$$

The variational formulation (22) for (w_1, r_1) with (w_2, r_2) as test functions shows that the right-hand side in (25) equals the same expression, up to exchanging w_1 and w_2. Hence, (25) holds true and T is self-adjoint. □

Theorem 3.6. *Assume that $\kappa \geq c > 0$ and $M \geq c > 0$ are strictly positive in D. Then the operator T is coercive on $(H^1(D)^d, \langle\cdot,\cdot\rangle_*)$.*

Proof. The definition of $\langle\cdot,\cdot\rangle_*$ in (19) and the definition of T in Theorem 3.4 imply that

$$\begin{aligned}\langle Th, h\rangle_* &= \int_D \big(D(Th){:}D(h) + h^\top M(Th)\big)\,\mathrm{d}x \\ &= \int_D \big(\kappa D(h-w){:}D(h) + h^\top M(h-w)\big)\,\mathrm{d}x\,.\end{aligned}$$

Obviously,

$$\int_D \kappa D(h-w){:}D(h)\,\mathrm{d}x \;= \int_D \kappa D(h-w){:}D(h-w)\,\mathrm{d}x \;+ \int_D \kappa D(h-w){:}D(w)\,\mathrm{d}x\,,$$

and

$$\int_D h^\top M(h-w)\,\mathrm{d}x \;= \int_D (h-w)^\top M(h-w)\,\mathrm{d}x \;+ \int_D w^\top M(h-w)\,\mathrm{d}x\,.$$

Now use (23) with $v = w$ to obtain that

$$\begin{aligned}\langle Th, h\rangle_* &= \int_D \kappa D(h-w){:}D(h-w)\,\mathrm{d}x \;+ \int_D \kappa D(h-w){:}D(w)\,\mathrm{d}x \\ &\quad + \int_D (h-w)^\top M(h-w)\,\mathrm{d}x \;+ \int_D w^\top M(h-w)\,\mathrm{d}x \\ &= \int_D \kappa D(h-w){:}D(h-w)\,\mathrm{d}x \;+ \int_D (h-w)^\top M(h-w)\,\mathrm{d}x \\ &\quad + \int_\Omega \mu_0 D(w){:}D(w)\,\mathrm{d}x \;- \int_\Omega r\,\mathrm{div}\, w\,\mathrm{d}x \;+ \int_\Gamma \alpha_\parallel |w_\parallel|^2\,\mathrm{d}S \\ &\quad + \int_\Gamma \alpha_\perp |w_\perp|^2\,\mathrm{d}S \;+ \int_\Omega q\,\mathrm{div}\, w\,\mathrm{d}x \qquad \forall q \in L^2(\Omega).\end{aligned} \tag{26}$$

Finally choosing the test function q to be r, (26) becomes

$$\begin{aligned}\langle Th, h\rangle_* &= \int_D \kappa D(h-w){:}D(h-w)\,\mathrm{d}x \;+ \int_D (h-w)^\top M(h-w)\,\mathrm{d}x \\ &\quad + \int_\Omega \mu_0 D(w){:}D(w)\,\mathrm{d}x \;+ \int_\Gamma \alpha_\parallel |w_\parallel|^2\,\mathrm{d}S \;+ \int_\Gamma \alpha_\perp |w_\perp|^2\,\mathrm{d}S\,.\end{aligned} \tag{27}$$

The task is now to estimate the terms of the right of (27). First,

$$\begin{aligned}\int_D \kappa D(h-w){:}D(h-w)\,\mathrm{d}x \;&\geq c_1 \int_D |D(h-w)|^2\,\mathrm{d}x\,, \\ \int_D (h-w)^\top M(h-w)\,\mathrm{d}S \;&\geq c_2 \int_D |h-w|^2\,\mathrm{d}S\,.\end{aligned}$$

Second, the coercivity of the bilinear form $a(\cdot,\cdot)$ on $H^1(\Omega)^d$ implies

$$\int_\Omega \mu_0 D(w){:}D(w)\,\mathrm{d}x \;+ \int_\Gamma \alpha_\parallel |w_\parallel|^2\,\mathrm{d}S \;+ \int_\Gamma \alpha_\perp |w_\perp|^2\,\mathrm{d}S \;\geq c_3 \|w\|^2_{H^1(\Omega)^d}.$$

Consequently,

$$\begin{aligned}\langle Th,h\rangle_* \geq& c_1\int_D |D(h-w)|^2\,\mathrm{d}x + c_2\int_D |h-w|^2\,\mathrm{d}x + c_3\int_D (|D(w)|^2+|w|^2)\,\mathrm{d}x\\ \geq& \int_D \Big[c_1|D(h)|^2 - 2c_1(D(h){:}D(w)) + (c_1+c_3)|D(w)|^2\Big]\,\mathrm{d}x\\ &+\int_D \Big[c_2|h|^2 - 2c_2hw + (c_2+c_3)|w|^2\Big]\,\mathrm{d}x\\ \geq& \int_D \Big[\big|\sqrt{c_1+c_3}\,D(w) - \frac{c_1\,D(h)}{\sqrt{c_1+c_3}}\big|^2 + c_1\Big(1-\frac{c_1}{c_1+c_3}\Big)|D(h)|^2\Big]\,\mathrm{d}x\\ &+\int_D \Big[\big|\sqrt{c_2+c_3}\,w - \frac{c_2}{\sqrt{c_2+c_3}}h\big|^2 + c_2\Big(1-\frac{c_2}{c_2+c_3}\Big)|h|^2\Big]\,\mathrm{d}x\\ \geq& \frac{c_1c_3}{\sqrt{c_1+c_3}}\|D(h)\|^2_{L^2(D)^{d\times d}} + \frac{c_2c_3}{\sqrt{c_2+c_3}}\|h\|^2_{L^2(D)^d} \geq c_4\|h\|^2_{H^1(D)^d}.\end{aligned}$$

□

Theorem 3.7. *The difference $\Lambda_0-\Lambda_1 : L^2(\Gamma)^d \to L^2(\Gamma)^d$ is compact, self-adjoint and non-negative. Its one-dimensional kernel is $\{g\in L^2(\Gamma)^d, g(x) = cn(x)$ for some $c\in\mathbb{R}\}$.*

Proof. The factorization $\Lambda_0-\Lambda_1 = H^*TH$ and the compactness of H^* imply that the difference $\Lambda_0-\Lambda_1$ is compact; Theorem 3.5 and the factorization yield the self-adjointness of the relative Robin-to-Dirichlet operator. The coercivity of T implies that $\langle(\Lambda_0-\Lambda_1)g,g\rangle_{L^2(\Gamma)^d}\geq 0$ for all $g\in L^2(\Gamma)^d$. Hence, $\Lambda_0-\Lambda_1$ is non-negative. Next, we prove the stated characterization of the kernel of $\Lambda_0-\Lambda_1$. Let $g\in L^2(\Gamma)^d$ with $(\Lambda_0-\Lambda_1)g=0$. Then

$$0 = \langle(\Lambda_0-\Lambda_1)g,g\rangle_{L^2(\Gamma)^d} = \langle H^*THg,g\rangle_{L^2(\Gamma)^d} = \langle THg,Hg\rangle_* \geq c\|Hg\|^2_{H^1(D)^d},$$

and so $Hg=0$. Let $0=Hg=u_0|_D$ where $(u_0,p_0)\in H^1(\Omega)^d\times L^2(\Omega)$ solve (15). From Lemma A.3 we deduce that $u_0=0$ in Ω and that p_0 is constant in Ω, say $p_0=-c\in\mathbb{R}$. Consequently, (15) implies that $c\int_\Omega \mathrm{div} v\,\mathrm{d}x = \int_\Gamma g^\top v\,\mathrm{d}S$ for all $v\in H^1(\Omega)^d$. Using the divergence theorem and a decomposition into tangential and normal components, we find that

$$c\int_\Gamma v_\perp\cdot n\,\mathrm{d}S = \int_\Gamma v_\parallel^\top g_\parallel\,\mathrm{d}S + \int_\Gamma v_\perp^\top g_\perp\,\mathrm{d}S \qquad \forall v\in H^1(\Omega)^d. \tag{28}$$

Choosing v such that $(v|_\Gamma)_\perp = 0$ on Γ shows that $g_\parallel=0$ on Γ. Hence, $\int_\Gamma v_\perp^\top(cn-g_\perp)\,\mathrm{d}S=0$ for arbitrary $v\in H^1(\Omega)^d$. Thus $g_\perp = cn$ and $\ker(\Lambda_0-\Lambda_1)\subset\{g=cn\}$.

Now we prove that $\{g=cn\}\subset\ker(\Lambda_0-\Lambda_1)$. We assume that $g=cn$ for some constant c. The pair $(u_0,p_0)=(0,c)$ solves (15) for boundary data $g_{\parallel,\perp}$. (This follows from the same computation as in the last part). Obviously, $Hg=0$, since u_0 vanishes on Ω. Since H and $\Lambda_0-\Lambda_1$ are related by the factorization of Theorem 3.4, we deduce that $(\Lambda_0-\Lambda_1)g=0$. □

Since the relative Robin-to-Dirichlet operator is a compact and self-adjoint operator, there exists a complete orthonormal eigensystem $(\lambda_l,\pi_l)_{l\in\mathbb{N}}$ of $\Lambda_0-\Lambda_1$ such that $\lambda_l\to 0$ as $l\to\infty$. Since $\Lambda_0-\Lambda_1$ is non-negative, it is obvious that $\lambda_l\geq 0$ and the characterization of the kernel of $\Lambda_0-\Lambda_1$ shows that precisely one eigenvalue vanishes. For simplicity, we define $\lambda_1=0$ to be the zero eigenvalue, and order the remaining eigenvalues $\lambda_2\geq\lambda_3\geq\cdots>0$ in decreasing order.

4. **Fundamental solution and Green's function of the Stokes equations.** The second important ingredient of the Factorization method is a characterization of the inclusion D via the Green's function of the Stokes equations. In this section, we construct this Green's function via a correction of the boundary values of the fundamental solution of the Stokes equations. To this end, we will assume that the viscosity μ_0 of the background medium is constant. Without loss of generality, we choose the simplest case,

$$\mu_0 = 2 \quad \text{in } \Omega,$$

since then $\operatorname{div}(\mu_0 D(u)) = \Delta u$ for any divergence-free function due to Lemma 2.1. It is not difficult to see that any other (positive) constant viscosity can be treated analogously by a simple scaling argument. The treatment of varying background viscosities requires more involved adaptions of the fundamental solution to get the Green's function for varying viscosity, see, e.g., [13] for the case of the Laplace equation.

The fundamental solution of the Stokes equations can be found in many references on boundary integral equations for the Stokes equations, see, e.g., [10, 19, 15]. We will concentrate in this section on the case $d = 2$ and announce the results for $d = 3$ in the end of the section without proof. For $x \neq y \in \mathbb{R}^2$, we set

$$S_{ij}(x,y) = \frac{1}{8\pi}\Big[\delta_{ij} \ln \frac{1}{|x-y|} + \frac{(x_i - y_i)(x_j - y_j)}{|x-y|^2}\Big], \quad s_i(x,y) = \frac{(x_i - y_i)}{2\pi\,|x-y|^2}.$$

The functions

$$S(x,y) = \begin{pmatrix} S_{11}(x,y) & S_{12}(x,y) \\ S_{21}(x,y) & S_{22}(x,y) \end{pmatrix} \quad \text{and} \quad s(x,y) = \begin{pmatrix} s_1(x,y) \\ s_2(x,y) \end{pmatrix}$$

are called the fundamental solution of the Stokes equations in two dimensions. We denote the two columns of the 2×2 matrix-valued function S by $S_1 = (S_{11}, S_{21})^\top$ and by $S_2 = (S_{12}, S_{22})^\top$. For $i = 1, 2$, one can explicitly compute that the pair (S_i, s_i) satisfies

$$\begin{aligned} -\Delta S_i(x,y) + \nabla s_i(x,y) &= 0 \qquad \text{for } x \neq y, \\ \operatorname{div} S_i(x,y) &= 0 \qquad \text{for } x \neq y. \end{aligned} \tag{29}$$

The Green's function is now defined to correct the inhomogeneous boundary values of the fundamental solution to homogeneous Robin boundary conditions. For $y \in \Omega$, define correction terms

$$R(x,y) = \begin{pmatrix} R_{11}(x,y) & R_{12}(x,y) \\ R_{21}(x,y) & R_{22}(x,y) \end{pmatrix} \quad \text{and} \quad r(x,y) = \begin{pmatrix} r_1(x,y) \\ r_2(x,y) \end{pmatrix},$$

where $R_{ij} \in H^1(\Omega)$, $R_i = (R_{1i}, R_{2i})^\top$, and $r_i \in L^2(\Omega)$. If, for $i = 1, 2$ and $y \in \Omega$, the pair $(R_i, r_i) \in H^1(\Omega)^2 \times L^2(\Omega)$ is a variational solution to the Stokes problem

$$-\Delta R_i(\cdot, y) + \nabla r_i(\cdot, y) = 0 \quad \text{and} \quad \operatorname{div} R_i(\cdot, y) = 0 \quad \text{in } \Omega, \tag{30}$$

subject to the boundary conditions

$$2D_\parallel(R_i(\cdot,y)) + \alpha_\parallel R_i(\cdot,y)_\parallel = -[2D_\parallel(S_i(\cdot,y)) + \alpha_\parallel S_i(\cdot,y)_\parallel] \qquad \text{on } \Gamma \tag{31}$$

and

$$\begin{aligned} (r_i(\cdot,y)n - 2D_\perp(R_i(\cdot,y))n) - \alpha_\perp R_i(\cdot,y)_\perp \\ = -[(s_i(\cdot,y)n - 2D_\perp(S_i(\cdot,y))n) - \alpha_\perp S_i(\cdot,y)_\perp] \qquad \text{on } \Gamma, \end{aligned} \tag{32}$$

then $(E, e) = (S, s) + (R, r)$ is called the Green's function for the Stokes equations in Ω. Note that all right-hand sides in the above boundary conditions for (R_i, r_i)

belong to $L^2(\Gamma)^2$, since the singularity $y \in \Omega$ of the fundamental solution is away from the boundary Γ. The explicit variational formulation defining (R_i, r_i) can be found from (13), choosing $\mu \equiv 2$, $M = 0$, $g_\parallel = -[\mu D_\parallel(S_i) + \alpha_\parallel(S_i)_\parallel]$ and $g_\perp = (s_i n - \mu D_\perp(S_i)) - \alpha_\perp(S_i)_\perp$.

Again, we emphasize that the 2×2 matrix-valued function E consists of the two columns E_1 and E_2. Obviously, the Green's function (E, e) solves, for $i = 1, 2$,

$$\begin{aligned} -\Delta E_i(\cdot, y) + \nabla e_i(\cdot, y) &= 0 \qquad \text{in } \Omega \setminus \{y\}, \\ \operatorname{div} E_i(\cdot, y) &= 0 \qquad \text{in } \Omega \setminus \{y\}, \\ 2D_\parallel(E_i(\cdot, y)) + \alpha_\parallel E_i(\cdot, y)_\parallel &= 0 \qquad \text{on } \Gamma, \\ (e_i(\cdot, y)n - 2D_\perp(E_i(\cdot, y))n) - \alpha_\perp E_i(\cdot, y)_\perp &= 0 \qquad \text{on } \Gamma. \end{aligned} \tag{33}$$

The following sampling function in two dimensions plays a main role for the construction of the Factorization method in the next section. For every $z \in \Omega$ and some $t \in [0, 2\pi)$ we define

$$\phi_z \in L^2(\Gamma)^2 \qquad \text{by} \qquad \phi_z := \cos(t)\, E_1(\cdot, z)|_\Gamma + \sin(t)\, E_2(\cdot, z)|_\Gamma\,. \tag{34}$$

The parameter t could in principle be chosen in dependence on the sampling point z. However, in all our numerical examples, we will always work with a fixed t, for simplicity. The sampling function ϕ_z characterizes the inclusion D via the range $\mathcal{R}(H^*)$ of the adjoint $H^* : L^2(D)^{2\times 2} \to L^2(\Gamma)^2$, see Theorem 3.2.

Theorem 4.1. *For $z \in \Omega$ it holds that $z \in D$ if and only if $\phi_z \in \mathcal{R}(H^*)$.*

Due to the divergence constraint for the velocity field, the proof of Theorem 4.1 is substantially more involved than the corresponding result for, e.g., the Laplace equation. The easy direction of the proof is based on the following auxiliary result that we will not prove in detail since the arguments are rather standard, see, e.g., [16].

Lemma 4.2. *For all $z \in \Omega$ and $t \in [0, 2\pi]$, the function defined by*

$$x \mapsto \cos(t)E_1(x, z) + \sin(t)E_2(x, z) \qquad \text{for } x \in \Omega \setminus \{z\}$$

does not belong to $H^1(\Omega)^2$.

In a nutshell, the proof of Lemma 4.2 follows from the definition of $E_i = S_i + R_i$, from the fact that $R_i \in H^1(\Omega)^2$ by definition, and from the singularity of S_i at $x = y$, which prevents ∇S_i from being square integrable in Ω. Admitting this result, we next prove Theorem 4.1.

Proof of Theorem 4.1. First, let $z \in D$. To show that ϕ_z belongs to the range of H^* we cut off the singularity of the Green's function E. This cut-off is usually done by multiplication of E with a smooth function that vanishes at the singularity. This is, however, not a successful approach here, since it destroys the divergence condition $\operatorname{div} E_{1,2}(\cdot, z) = 0$. Instead, we construct a pre-image of ϕ_z using a vector potential approach: It is easy to see that $P_{1,2}(x) : \mathbb{R}^2 \setminus \{0\} \to \mathbb{R}$ defined by

$$P_1(x) = x_2 \log(|x|) - x_2 \quad \text{and} \quad P_2(x) = x_1 \log(|x|) - x_1,$$

satisfies

$$S_i(x - y) = -\frac{1}{4\pi} \begin{pmatrix} -\frac{\partial P_i(x-y)}{\partial x_2} \\ \frac{\partial P_i(x-y)}{\partial x_1} \end{pmatrix}, \quad x \neq y,\ i = 1, 2.$$

Let us choose a closed disc $K_\varepsilon(z) = \{x \in \mathbb{R}^2 : |x - z| \leq \varepsilon\}$ with center z and radius ε such that $K_\varepsilon(z) \subset D$. In addition, choose a cut-off function $\varphi \in C^\infty(\mathbb{R}^2)$ such

that $\varphi(x) = 0$ for $|x-z| \leq \varepsilon/2$ and $\varphi(x) = 1$ for $|x-z| \geq \varepsilon$. Using the cut-off function φ, we define $v \in H^1(\Omega)^2$ by

$$v(x) = -\frac{1}{4\pi}\left[\cos(t)\begin{pmatrix} -\frac{\partial}{\partial x_2}(\varphi(x)P_1(x-y)) \\ \frac{\partial}{\partial x_1}(\varphi(x)P_1(x-y))\end{pmatrix} + \sin(t)\begin{pmatrix} -\frac{\partial}{\partial x_2}(\varphi(x)P_2(x-y)) \\ \frac{\partial}{\partial x_1}(\varphi(x)P_2(x-y))\end{pmatrix}\right] + \cos(t)R_1(x,z) + \sin(t)R_2(x,z), \quad x \in \Omega. \tag{35}$$

The terms in the first line of (35) are smooth functions of x because $x \mapsto \varphi(x)P_i(x-y)$ is smooth. Note also that v is divergence-free in Ω by construction via the vector potentials. Next, we define a corresponding pressure $q \in L^2(\Omega)$ by $q(x) := \varphi(x)[\cos(t)e_1(x,z)+\sin(t)e_2(x,z)]$ for $x \in \Omega$. Then $(v,q) \in H^1(\Omega)^2 \times L^2(\Omega)$ satisfies the Stokes equations in $\Omega \setminus \overline{D}$, and Lemma 2.2 implies that

$$\begin{aligned} &2\int_{\Omega\setminus\overline{D}} D(v){:}D(\psi)\,\mathrm{d}x + \int_\Gamma \alpha_\parallel v_\parallel \psi_\parallel \,\mathrm{d}S + \int_\Gamma \alpha_\perp v_\perp \psi_\perp \,\mathrm{d}S \\ &- \int_{\Omega\setminus\overline{D}} q\,\mathrm{div}\,\psi\,\mathrm{d}x + \int_{\Omega\setminus\overline{D}} \theta\,\mathrm{div}\,v\,\mathrm{d}x - \int_{\partial D} \psi^\top(qn - 2D(v)n)\,\mathrm{d}S = 0 \\ &\qquad\qquad \forall \psi \in H^1(\Omega\setminus\overline{D})^2,\ \forall \theta \in L^2(\Omega\setminus\overline{D}). \end{aligned} \tag{36}$$

Note that the boundary term on ∂D is well-defined since $\psi|_\Gamma \in H^{1/2}(\Gamma)^2$ and since $qn - 2D(v)n \in H^{-1/2}(\Gamma)^2$ due to $-\mathrm{div}(2D(v)) + \nabla q \in L^2(\Omega)^2$, compare [21, Chapter 4]. Recall the definition of the inner product $\langle\cdot,\cdot\rangle_*$ on $H^1(D)^2$ from (19). Riesz's lemma implies that there exists a unique solution $u \in H^1(D)^2$ to

$$\begin{aligned} \langle u, \psi\rangle_* &= 2\int_D D(v){:}D(\psi)\,\mathrm{d}x \\ &\quad - \int_D q\,\mathrm{div}\,\psi\,\mathrm{d}x + \int_{\partial D} \psi^\top(qn - 2D(v)n)\,\mathrm{d}S \quad \forall \psi \in H^1(D)^2. \end{aligned} \tag{37}$$

Adding (37) and (36) for $\theta = 0$, we get that

$$\begin{aligned} &2\int_\Omega D(v){:}D(\psi)\,\mathrm{d}x + \int_\Gamma \alpha_\parallel v_\parallel \psi_\parallel \,\mathrm{d}S + \int_\Gamma \alpha_\perp v_\perp \psi_\perp \,\mathrm{d}S - \int_\Omega q\,\mathrm{div}\,\psi\,\mathrm{d}x \\ &\qquad = \langle u, \psi\rangle_* = \int_D \kappa D(u){:}D(\psi)\,\mathrm{d}x + \int_D \psi^\top M u\,\mathrm{d}x \qquad \forall \psi \in H^1(\Omega)^2. \end{aligned}$$

Since v has been constructed such that $\mathrm{div}\,v = 0$, the last equation obviously implies that

$$\begin{aligned} &2\int_\Omega D(v){:}D(\psi)\,\mathrm{d}x + \int_\Gamma \alpha_\parallel v_\parallel \psi_\parallel \,\mathrm{d}S + \int_\Gamma \alpha_\perp v_\perp \psi_\perp \,\mathrm{d}S \\ &- \int_\Omega q\,\mathrm{div}\,\psi\,\mathrm{d}x + \int_\Omega \theta\,\mathrm{div}\,v\,\mathrm{d}x = \int_D \kappa D(u){:}D(\psi)\,\mathrm{d}x + \int_D \psi^\top M u\,\mathrm{d}x \\ &\qquad\qquad \forall \psi \in H^1(\Omega)^2,\ \forall \theta \in L^2(\Omega). \end{aligned} \tag{38}$$

Therefore, Theorem 3.2 shows that $H^*(u|_D) = v|_\Gamma = \phi_z$ and thus $\phi_z \in \mathcal{R}(H^*)$.

Second, let $z \notin D$. We have to show that ϕ_z is not contained in the range of H^* and we argue by contradiction: Suppose that $\phi_z = H^*h$ for some $h \in H^1(D)^2$. Let $(u,p) \in H^1(\Omega)^2 \times L^2(\Omega)$ be the solution to (20) such that $H^*(h) = u|_\Gamma$. Additionally,

set $D_\varepsilon = D \cup \{x \in \Omega,\ |x-z| < \varepsilon\} \subset \Omega$ and define

$$w = u - [\cos(t)(E_1(\cdot,z) + \sin(t)E_2(\cdot,z)] \qquad \text{in } \Omega \setminus \overline{D}_\varepsilon(z)$$
$$s = p - [\cos(t)e_1(\cdot,z) + \sin(t)e_2(\cdot,z)] \qquad \text{in } \Omega \setminus \overline{D}_\varepsilon(z).$$

Then $(w,s) \in H^1(\Omega \setminus \overline{D}_\varepsilon(z))^2 \times L^2(\Omega \setminus \overline{D}_\varepsilon(z))$ and $w|_\Gamma \in L^2(\Gamma)^2$ satisfies that

$$w|_\Gamma = u|_\Gamma - \Big[\cos(t)E_1(\cdot,z)|_\Gamma + \sin(t)E_2(\cdot,z)|_\Gamma\Big] = u|_\Gamma - \phi_z. = H^*h - \phi_z = 0.$$

In addition, $(u,p) \in H^1(\Omega)^2 \times L^2(\Omega)$ solves (20), that is, for every $\varepsilon > 0$ it holds that $(w,s) \in H^1(\Omega \setminus \overline{D}_\varepsilon(z))^2 \times L^2(\Omega \setminus \overline{D}_\varepsilon(z))$ is by construction a variational solution to

$$\begin{aligned} -2\operatorname{div} D(w) + \nabla s = 0 \quad \text{and} \quad \operatorname{div} w = 0 \qquad & \text{in } \Omega\setminus\overline{D}_\varepsilon(z), \\ 2D_\parallel(w) + \alpha_\parallel w_\parallel = 0 \qquad & \text{on } \Gamma, \\ (sn - 2D_\perp(w)) - \alpha_\perp w_\perp = 0 \qquad & \text{on } \Gamma. \end{aligned}$$

Since, $w|_\Gamma = 0$ we conclude that $2D_\perp(w)n - sn$ and $D_\parallel(w)$ vanish on Γ, too. Hence, the unique continuation result stated in Lemma A.4 and extension by zero outside Ω imply that w vanishes in $\Omega\setminus\overline{D}_\varepsilon(z)$ for any $\varepsilon > 0$. Since $\varepsilon > 0$ was arbitrary,

$$u = \cos(t)E_1(\cdot,z) + \sin(t)E_2(\cdot,z) \qquad \text{in } \Omega\setminus\{z\}. \tag{39}$$

By construction, $u \in H^1(\Omega)^2$. Lemma 4.2 states that the right-hand side in (39) does not belong to $H^1(\Omega)^2$, which yields a contradiction. □

Remark 4. For $d = 3$, all results stated in this section remain correct, but the proofs partly have to be adapted. Of course, the fundamental solution takes a different form, see, e.g., [24, 19, 15]. The fundamental solution (S,s) is defined via the functions

$$S_{ij}(x,y) = \frac{1}{16\pi}\Big[\delta_{ij}\frac{1}{|x-y|} + \frac{(x_i-y_i)(x_j-y_j)}{|x-y|^3}\Big], \qquad s_i(x,y) = -\frac{(x_i-y_i)}{4\pi\,|x-y|^3},$$

for $x \neq y \in \mathbb{R}^3$ and $i,j = 1,2,3$. The Green's function $(E,e) = (S,s) + (R,r)$ is constructed precisely as in (30–32). The sampling function ϕ_z is again defined as a (non-trivial) linear combination of the three columns $E_{1,2,3}$ of the Green's function,

$$\phi_z = \zeta_1 E_1(\cdot,z)|_\Gamma + \zeta_2 E_2(\cdot,z)|_\Gamma + \zeta_3 E_3(\cdot,z)|_\Gamma \quad \text{for } z \in \Omega \text{ and } \zeta \in \mathbb{R}^3 \text{ with } |\zeta| = 1. \tag{40}$$

The two-dimensional vector potential used in the proof of Theorem 4.1 has to be replaced by a corresponding three-dimensional construction that can be found in, e.g., [24]. The rest of the proof essentially remains the same, up to adapting the space dimension.

5. **The factorization method.** Theorem 4.1 explicitly characterizes the inclusion $D \subset \Omega$ using the range of the operator H^*. This operator is, however, unknown because it cannot be computed without knowing the inclusion D. Fortunately, the factorization $\Lambda_0 - \Lambda_1 = H^*TH$ from Theorem 3.4 relates H^* with the known data $\Lambda_0 - \Lambda_1$. A range identity will then provide to a characterization of the inclusion D in terms of $\Lambda_0 - \Lambda_1$ in the main result of this paper, see Theorem 5.1.

We exploit the eigendecomposition

$$(\Lambda_0 - \Lambda_1)g = \sum_{l=1}^{\infty} \lambda_l \langle g, \pi_l\rangle_{L^2(\Gamma)^d}\pi_l, \qquad g \in L^2(\Gamma)^d,$$

of $\Lambda_0 - \Lambda_1$ from Theorem 3.7 to define the (positive semi-definite) square root

$$(\Lambda_0 - \Lambda_1)^{1/2} g := \sum_{l=1}^{\infty} \sqrt{\lambda_l} \langle g, \pi_l \rangle \pi_l, \qquad g \in L^2(\Gamma)^d.$$

This square root is again a bounded self-adjoint operator on $L^2(\Gamma)^d$ and

$$(\Lambda_0 - \Lambda_1)^{1/2}((\Lambda_0 - \Lambda_1)^{1/2} g) = \sum_{l=1}^{\infty} (\sqrt{\lambda_l})^2 \langle g, \pi_l \rangle \pi_l = (\Lambda_0 - \Lambda_1) g.$$

Now we have two factorizations

$$\Lambda_0 - \Lambda_1 = H^* T H = (\Lambda_0 - \Lambda_1)^{1/2} (\Lambda_0 - \Lambda_1)^{1/2}$$

of the relative Robin-to-Dirichlet operator on $L^2(\Gamma)^d$. Since T is self-adjoint and coercive, we can apply the range characterization from [17, Lemma 5.15] (see Lemma A.5 in the appendix) to the first factorization. The result is that for any $0 \neq \phi \in L^2(\Gamma)^d$ there holds

$$\phi \in \mathcal{R}(H^*) \Leftrightarrow \inf\{ \langle (\Lambda_0 - \Lambda_1) g,\, g \rangle_{L^2(\Gamma)^d} : g \in L^2(\Gamma)^d,\, \langle g, \phi \rangle_{L^2(\Gamma)^d} = 1 \} > 0. \tag{41}$$

Applying the same result to the second factorization $\Lambda_0 - \Lambda_1 = (\Lambda_0 - \Lambda_1)^{1/2}(\Lambda_0 - \Lambda_1)^{1/2}$ we deduce that for any $0 \neq \phi \in L^2(\Gamma)^d$ there holds

$$\phi \in \mathcal{R}((\Lambda_0 - \Lambda_1)^{1/2}) \Leftrightarrow \inf\{ \langle (\Lambda_0 - \Lambda_1) g, g \rangle_{L^2(\Gamma)^d} : g \in L^2(\Gamma)^d,\, \langle g, \phi \rangle_{L^2(\Gamma)^d} = 1 \} > 0. \tag{42}$$

Together, (41) and (42) imply the range identity

$$\mathcal{R}((\Lambda_0 - \Lambda_1)^{1/2}) = \mathcal{R}(H^*). \tag{43}$$

Since $(\lambda_l, \pi_l)_{l \in \mathbb{N}}$ is an eigensystem of $\Lambda_0 - \Lambda_1$ and since $\lambda_l \geq 0$, it is obvious that $(\sqrt{\lambda_l}, \pi_l)_{l \in \mathbb{N}}$ is an eigensystem of $(\Lambda_0 - \Lambda_1)^{1/2}$. Picard's range criterion [17, Theorem A.54] then implies the following characterization of D via the sampling functions ϕ_z defined in (34) and in (40) for the case of dimension two and three, respectively.

Theorem 5.1. *(Factorization method) For any point $z \in \Omega$ it holds that*

$$z \in D \Longleftrightarrow \sum_{l=2}^{\infty} \frac{|(\phi_z, \pi_l)_{L^2(\Gamma)^d}|^2}{\lambda_l} < \infty. \tag{44}$$

Proof. Theorem 4.1 and the range identity (43) imply that $z \in D$ if and only if $\phi_z \in \mathcal{R}((\Lambda_0 - \Lambda_1)^{1/2})$. Recall that in last paragraph of Section 3 we have set $\lambda_1 = 0$, such that the first eigenfunction π_1 spans the kernel of $(\Lambda_0 - \Lambda_1)^{1/2}$. Moreover, since ϕ_z is the trace of a linear combination of the divergence-free columns $E_{1,\dots,d}(\cdot, z)$ of the Green's function, the divergence theorem states that $\int_\Gamma n \cdot \phi_z \, \mathrm{d}S = 0$. In consequence, the characterization of the kernel of $\Lambda_0 - \Lambda_1$ implies that $\langle \phi_z, \pi_1 \rangle_{L^2(\Gamma)^d} = 0$. Thus,

$$\phi_z \in \operatorname{span}(\pi_1)^{\perp} = \overline{\mathcal{R}((\Lambda_0 - \Lambda_1)^{1/2})} \qquad \text{for all } z \in \Omega.$$

Hence, Picard's lemma shows that the series on the right of (44) is finite if and only if $\phi_z \in \mathcal{R}((\Lambda_0 - \Lambda_1)^{1/2})$, that is, if and only if $z \in D$. ∎

6. **Numerical examples.** In this section we present numerical experiments illustrating the theoretical results of the last sections and the feasibility of the method. We present images that are computed from relatively few normal measurements that are additionally perturbed by additive noise. For simplicity, all examples are two-dimensional. Further, all experiments are computed using synthetic data computed by a mixed finite element method based on Taylor-Hood ($\mathbb{P}2/\mathbb{P}1$) elements, see, e.g., [8, 6]. All finite element simulations are done using the `C++`-based open source finite element code FreeFem++ (see `www.freefem.org/ff++`).

For our numerical examples we decompose the boundary of the domain Ω into N connected pieces Γ_j, $j = 1, \dots, N$ of equal length and approximate functions on the boundary by piecewise constant (vector-valued) functions. We will denote this approximation space by $X^{(N)}$; later on, we will always choose $N = 16$. This rather low-dimensional choice is motivated by the difficulty to experimentally measure many degrees of freedom of a boundary flow in practice. Valves to measure or control the in- and outflow require sufficiently large holes in the boundary of the domain and cannot easily be shifted. Note that the mesh of the domain that we use to compute the synthetic data has many degrees of freedom on each boundary piece such that mean-value projections have to be used to project the boundary values of general finite-element functions into $X^{(N)}$. It is by the way not necessary that the boundary pieces cover the entire boundary, even if in all our examples this will be the case.

To approximate the difference $\Lambda_0 - \Lambda_1$, we firstly discretize (15) using Taylor-Hood elements to evaluate $Hg = u_0|_D$ on D, for all $g \in X^{(N)}$. Secondly, we exploit that $(\Lambda_0 - \Lambda_1)g = GHg$, inserting $(Hg)|_D$ in the right-hand side of the discretization of (18). Projecting the boundary values of the solution into $X^{(N)}$ yields a matrix representation $(\Lambda_0 - \Lambda_1)^{(N)}$ of $\Lambda_0 - \Lambda_1$ of dimension $dN \times dN$ (that is, a 32 matrix if $d = 2$ and $N = 16$). The eigenvalues and vectors of the self-adjoint and non-negative matrix $(\Lambda_0 - \Lambda_1)^{(N)}$ are $\lambda_j^{(N)} \geq 0$ and $\pi_j^{(N)} \in (\mathbb{R}^d)^N$ for $j = 1, \dots, dN$.

In our computational examples the domain Ω is the unit circle and the inclusion D consists of two disjoint circles of radius 0.1 centered in $(0, 0.3)^\top$ and in $(0.3, -0.3)^\top$. The background viscosity equals $\mu_0 \equiv 2$ and $\mu = 100$ and 2 inside and outside the inclusion D, respectively. The (scalar) material parameter M equals 50 inside the inclusion and vanishes outside. At first glance, these values seem rather big. However, Figure 1(a) shows that the resulting inclusion is well penetrated by a flow that is generated by an inflow on the right and an outflow on the left. The boundary parameters for this example, as well as for all the following ones are $\alpha_\parallel = 5$ and $\alpha_\perp = 10$. Moreover, the plot of the first component of this flow in Figure 1(b) shows that the velocity field is influenced by the inclusion. Of course, this influence decreases if one decreases the contrast; when setting, e.g., $\mu = 10$ and $M = 5$ inside D, the flow is no longer visibly influenced.

For the configuration explained in the last paragraph, the eigenvalues of the numerical approximation to $(\Lambda_0 - \Lambda_1)^{(16)}$ that we use for our inversion experiments are shown (in decreasing order) in Figure 1(c). The fact that one eigenvalue of $\Lambda_0 - \Lambda_1$ vanishes is reflected by the large gap in magnitude between the smallest eigenvalue (roughly equal to $5e - 18$) and all other eigenvalues. Of course, the precision of the computed eigenvalues depends on the spatial discretization of Ω. We test this precision by plotting the largest eigenvalue for different meshes in Figure 1(d). The parameter on the horizontal axis, say k, describes the maximal mesh width $h_k = \pi/(8k)$. We observe convergence of the largest eigenvalue as k

increases: 2, 3, and 4 correct digits are attained for $k = 6$, 11, and 22, respectively. We use $k = 12$ for generating the synthetic data later on.

Since the Green's function of the Stokes equations in Ω has in general no explicit representation we first compute the correction term (R, r) by discretizing (30–32). Second, we compute the Green's function by adding the (analytic evaluation) of the fundamental solution function and the numerical approximation to the correction term to construct the sampling function ϕ_z from (34). Computing the Green's function requires a finer mesh than computing the synthetic data, at least when the sampling point is close to the boundary. We found that $k = 39$ gives sufficient accuracy for reasonable images. Despite we could in principle compute testfunctions ϕ_z for several dipole directions (parametrized by t in (34)) we restrict ourselves to fix $t = 0$. Improving the reconstruction quality by, e.g., averaging or optimizing over dipole directions might be possible; our aim here is merely to give a proof of concept for the method.

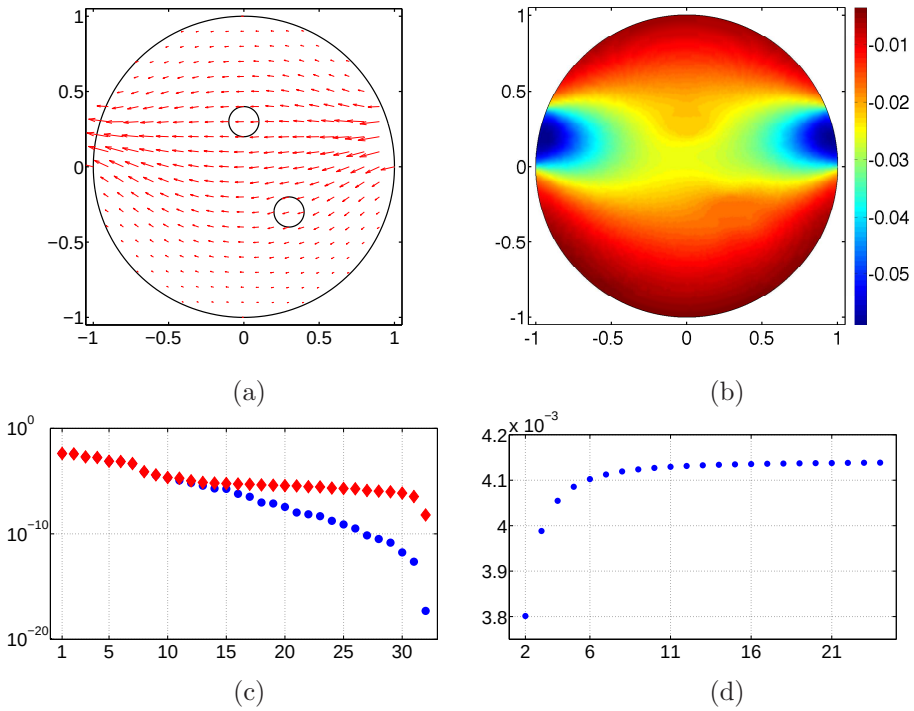

FIGURE 1. (a) Red arrows: velocity field for an inflow on the right and outflow on the left. Black lines indicate the domain and its inclusions. (b) The first component of the velocity field shown in (a). (c) Blue dots: the 32 eigenvalues of $(\Lambda_0 - \Lambda_1)^{(16)}$ (no artificial noise was added to the data). Red diamonds: 32 singular values of a random additive perturbation of $(\Lambda_0 - \Lambda_1)^{(16)}$, the relative noise level equals 1%. (d) Blue dots: the largest eigenvalue of $(\Lambda_0 - \Lambda_1)^{(16)}$ computed on different meshes. The eigenvalues are plotted against an integer k determining the mesh width $h_k = \pi/(8k)$.

The sampling points z determining the sampling function ϕ_z are chosen on a uniform grid $\mathcal{G}$ of Ω. We compute the sampling function ϕ_z from (34) for every sampling point (*without* projecting the boundary data of the fundamental solution into $X^{(N)}$). Note that this requires to solve the auxiliary problem (30–32) once for every sampling point. However, the sampling function does not depend on the inclusion and can be precomputed and re-used for several reconstructions in the same setting. After assembling the sampling function ϕ_z we project the result into $X^{(N)}$ using a mean-value projection and define

$$\phi_z^{(N)} = \big(\mathrm{vol}(\Gamma_j)^{-1} \textstyle\int_{\Gamma_j} \phi_z \, \mathrm{d}S \big)_{j=1}^N \in (\mathbb{R}^2)^N.$$

Tangential and normal components $\phi_{z,\parallel}^{(N)}$ and $\phi_{z,\perp}^{(N)}$ of $\phi_z^{(N)}$ are then defined componentwise as in (6).

Finally, to identify an inclusion D in a domain Ω we approximate the reciprocal of the function from (44) by

$$z \mapsto \left[\sum_{l=N_-}^{N_+} \big| \langle \phi_z^{(N)}, \pi_l^{(N)} \rangle_{(\mathbb{R}^2)^N} \big| / \lambda_l^{(N)} \right]^{-1}, \qquad z \in \mathcal{G}, \tag{45}$$

where $1 \le N_- < N_+ \le dN - 1$ are truncation indices. Roughly speaking, if the approximation quality of our discrete data is good enough, then Theorem 5.1 motivates that this procedure yields an image of the inclusion, since the function in (45) should be small outside D while taking large values inside D. Of course, the quality of the discrete data determines the resolution and the contrast of the resulting image.

In our numerical experiments, we noted that the tangential component of the measurements $\Lambda_0 - \Lambda_1$ is fairly small, usually about two orders of magnitude smaller than the normal component. This observation holds both for tangential and normal boundary excitations. To this end, in our subsequent examples we merely take the "normal" part of $\Lambda_0 - \Lambda_1$ as data, that is, we only use normal excitations and only measure the normal component of the trace of the resulting flow. Denote by $X_\perp^{(N)} = \{g \in X^{(N)},\, g \cdot n = 0 \text{ on } \Gamma\}$ the space of tangential vector fields in $X^{(N)}$. Replacing the space $X^{(N)}$ in the above construction of $(\Lambda_0 - \Lambda_1)^{(N)}$ we obtain a corresponding matrix representation $(\Lambda_0 - \Lambda_1)_{\perp\perp}^{(N)}$ of size $N \times N$. If we denote by $\lambda_{\perp,j}^{(N)}$ and $\pi_{\perp,j}^{(N)}$, the corresponding eigenvalues and vectors, the indicator function that we plot is hence

$$z \mapsto W_\perp(z) := \left[\sum_{l=N_-}^{N_+} \big| \langle \phi_{z,\perp}^{(N)}, \pi_{\perp,l}^{(N)} \rangle_{(\mathbb{R}^2)^N} \big| / \lambda_{\perp,l}^{(N)} \right]^{-1}, \qquad z \in \mathcal{G}. \tag{46}$$

In our experiments, the reconstructions obtained merely from normal measurements gave better results than those obtained from all measurements. This is presumably due to the large difference in magnitude of the normal and tangential data, which causes the tangential measurements to be inexact even when no artificial noise has been added. It made relatively little difference whether the excitations were chosen normally or tangentially, as long as we took normal measurements of the velocity field. Such normal measurements are, by the way, much simpler to measure reliably in a practical experiment.

In our implementation, we actually replace the factor $1/\lambda_{\perp,l}^{(N)}$ in (46) by $1/(\lambda_{\perp,l}^{(N)} + 2\epsilon)$ where $\epsilon > 0$ corresponds to the relative noise level, to avoid division by zero.

(There are definitely more sophisticated numerical techniques for regularizing the Picard series, see, e.g., [11, 12].) In our numerical experiments we noted that the image quality can be significantly improved by taking the freedom to vary both indices $N_\pm$. For the images shown in Figure 2 we always chose $N_- = 10$ and $N_+ = 15$. This choice produced the best overall results.

Figures 2(b,c,d) show the images of the inclusion D using $W_\perp(z)$ from synthetic data $(\Lambda_0 - \Lambda_1)^{(16)}_{\perp\perp}$ generated in the setting explained above. In Figures 2(c,d) we added a random matrix (generated using uniformly distributed random variables) to the discretization of $\Lambda_0 - \Lambda_1$. The noise was scaled such that the relative noise level equals 1% in (c) and 5% in (d). The experiments show that the method is able to separate the two inclusions up to a noise level of about 1%. However, even without artificial noise, the shape of the two inclusions is not reconstructed correctly, in contrast to position and size. This might be surprising when compared to reconstructions in impedance tomography, see, e.g., [11], but is probably due to the coarse approximation space $X^{(16)}$ that we employ for approximating functions on the boundary. The separation of the two inclusions is lost when the noise level increases to 5%, but geometric information on the inclusions can still be deduced from the corresponding image.

Appendix A. **Auxiliary results.** As in the main part of this text, Ω is a Lipschitz domain with boundary Γ. The following trace theorem is a well-known analytic tool, see, e.g., [21, 9].

Theorem A.1. *There exists a bounded linear operator $\gamma : H^1(\Omega) \to L^2(\Gamma)$ such that $\|\gamma u\|_{L^2(\Gamma)} \leq C(\Omega)\|u\|_{H^1(\Omega)}$ for each $u \in H^1(\Omega)$ and $\gamma u = u|_\Gamma$ if $u \in H^1(\Omega) \cap C(\bar{\Omega})$. We call γu the trace of u on Γ. The trace operator γ is compact from $H^1(\Omega)$ into $L^2(\Gamma)$.*

Note that we do not denote the trace operator explicitly in this text, but rather write $u|_\Gamma$. Often, we even omit to denote the trace operation completely if it follows from the context (as, e.g., inside boundary integrals). For the following Korn's inequalities, we refer to, e.g., [20, 21, 6].

Lemma A.2. *(Korn's inequalities) (a) There exists $c > 0$ such that*

$$\int_\Omega |D(u)|^2 \,\mathrm{d}x + \int_\Omega |u|^2 \,\mathrm{d}x \geq c\|u\|^2_{H^1(\Omega)^d} \qquad \forall u \in H^1(\Omega)^d.$$

(b) For a non-empty subdomain $D \subset \Omega$ there exists $c > 0$ such that

$$\int_\Omega |D(u)|^2 \,\mathrm{d}x + \int_D |u|^2 \,\mathrm{d}x \geq c\|u\|^2_{H^1(\Omega)^d} \qquad \forall u \in H^1(\Omega)^d.$$

(c) There exists $c > 0$ such that

$$\int_\Omega |D(u)|^2 \,\mathrm{d}x + \int_\Gamma \left(|u_\parallel|^2 + |u_\perp|^2\right) \,\mathrm{d}S \geq c\|u\|^2_{H^1(\Omega)^d} \qquad \forall u \in H^1(\Omega)^d.$$

The following lemma from [1, Proposition 2.1] states a unique continuation property for solutions to the Stokes equations.

Lemma A.3. *(Unique continuation property) Let D be an open, non-empty subset of Ω. If $(u, p) \in H^1(\Omega)^d \times L^2(\Omega)$ is a variational solution to*

$$-\Delta u + \nabla p = 0 \quad \text{in } \Omega \qquad \text{and} \qquad \operatorname{div} u = 0 \quad \text{in } \Omega,$$

and if $u = 0$ in D, then $u = 0$ in Ω and p is constant in Ω.

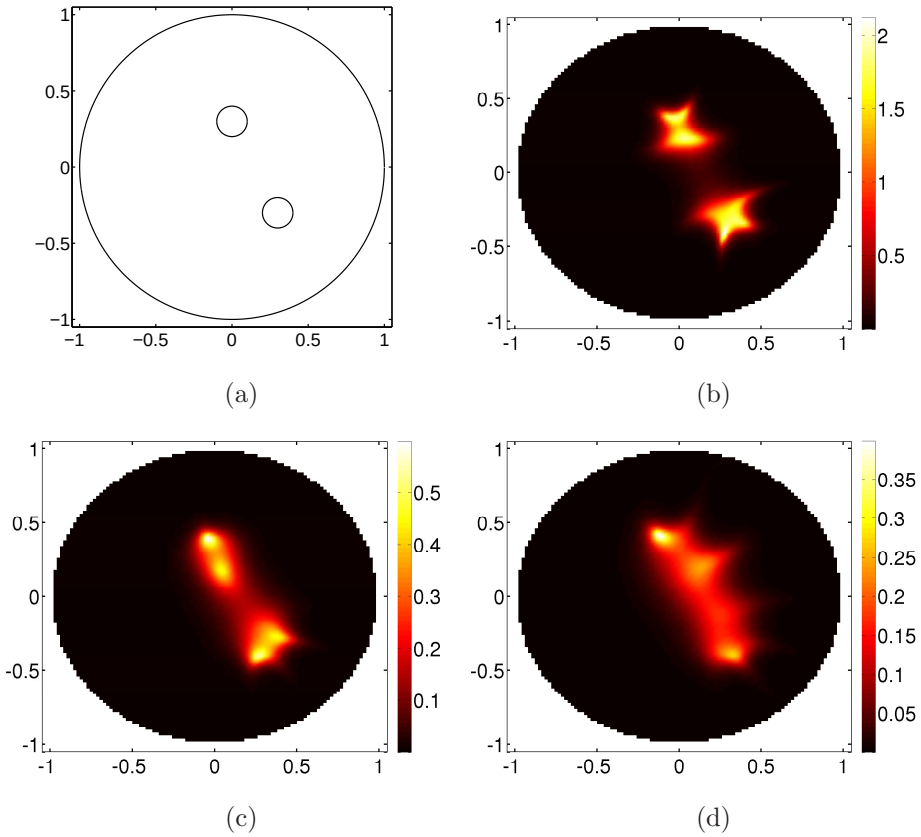

FIGURE 2. Images of the inclusion shown in (a) via plots of the function $W_\perp$ from (46) for $N_- = 10$ and $N_+ = 15$. (b) No artificial noise added to the synthetic data $\Lambda_0 - \Lambda_1$. (c) Artificial noise level of 1%. (d) Artificial noise level of 5%.

We recall that $(u, p) \in H^1(\Omega)^d \times L^2(\Omega)$ is a variational solution to the Stokes equations if

$$2\int_\Omega D(u){:}D(v)\,\mathrm{d}x \;-\int_\Omega p\,\mathrm{div}\,v\,\mathrm{d}x \;+\int_\Omega q\,\mathrm{div}\,u\,\mathrm{d}x \;=0$$

for all $v \in H^1(\Omega)^d$ and $q \in L^2(\Omega)$ with compact support in Ω. This variational formulation can of course also be formulated using ∇u instead of the deformation tensor $D(u)$ due to Lemma 2.1.

The next lemma extends the analytic continuation result from [17, Lemma 6.13] from the Helmholtz equation to the Stokes equations. The main tool to generalize the latter result are Green's first and second identity for the Stokes equations, see, e.g., [15, Chapter 2.3].

Lemma A.4. *Assume that Ω consists of two disjoint Lipschitz subdomains, $\bar\Omega = \bar\Omega_1 \cup \bar\Omega_2$ such that $\Omega_1 \cap \Omega_2 = \emptyset$. For $j = 1, 2$, let $u_j \in H^1(\Omega_j)^d$ and $p_j \in L^2(\Omega_j)$ be*

variational solutions to the Stokes equations

$$-\Delta D(u_j) + \nabla p_j = 0 \quad \text{in } \Omega_j \qquad \text{and} \qquad \operatorname{div} u_j = 0 \quad \text{in } \Omega_j.$$

Denote by $\Gamma := \partial\Omega_1 \cap \partial\Omega_2$ *the common boundary of* Ω_1 *and* Ω_2 *and let* $u_1 = u_2$ *in* $H^{1/2}(\Gamma)^d$ *and* $2D(u_1)n - p_1 n = 2D(u_2)n - p_2 n$ *in* $H^{-1/2}(\Gamma)^d$*, where* n *is a exterior unit normal vector to* Ω*. Define*

$$u(x) = \begin{cases} u_1(x), & x \in \Omega_1, \\ u_2(x), & x \in \Omega_2, \end{cases} \quad \text{and} \quad p(x) = \begin{cases} p_1(x), & x \in \Omega_1, \\ p_2(x), & x \in \Omega_2. \end{cases}$$

Then u *can be extended to an analytic function in* Ω *and* (u, p) *satisfies the Stokes equations in* Ω*.*

The next lemma is a well-known characterization of certain operator ranges, see, e.g., [17, Lemma 5.15].

Lemma A.5. *(Inf-criterion) Let* X *and* Y *be Hilbert spaces,* $B : X \to X$*,* $A : X \to Y$*, and* $T : Y \to Y$ *linear and bounded such that* $B = A^*TA$*. Furthermore, let* T *be self-adjoint and coercive, i.e.,* $\langle Ty, y\rangle_Y \geq c\|y\|_Y^2$ *for all* $y \in Y$*. Then it holds for any* $0 \neq \varphi \in X$ *that*

$$\varphi \in \mathcal{R}(A^*) \Leftrightarrow \inf\{\langle Bx, x\rangle_X : x \in X, \langle x, \varphi\rangle_X = 1\} > 0.$$

REFERENCES

[1] C. Alvarez, C. Conca, L. Friz, O. Kavian and J. H. Ortega, Identification of immersed obstacles via boundary measurements, *Inverse Problems*, **21** (2005), 1531–1552.

[2] C. J. Alves, R. Kress and A. L. Silvestre, Integral equations for an inverse boundary value problem for the two-dimensional stok *Journal of Inverse and Ill-Posed Problems*, **15** (2007), 461–481.

[3] A. Ben Abda, M. Hassine, M. Jaoua and M. Masmoudi, Topological sensitivity analysis for the location of small cavities in stokes flows. *SIAM Journal on Control and Optimization*, **48** (2009), 2871–2900.

[4] A. Ballerini, Stable determination of a body immersed in a fluid: The nonlinear stationary case, *Applicable Analysis*, **92** (2013), 460–481.

[5] M. Badra, F. Caubet and M. Dambrine, Detecting an obstacle immersed in a fluid by shape optimization methods, *M3AS*, **21** (2011), 2069–2101.

[6] S. C. Brenner and L. R. Scott, *The Mathematical Theory of Finite Element Methods*, Springer Verlag, New York, 2008.

[7] C. Conca, M. Malik and A. Munnier, Detection of a moving rigid solid in a perfect fluid, *Inverse Problems*, **26** (2010), 095010.

[8] A. Ern and J. L. Guermond, *Theory and Practice of Finite Elements*, Springer Verlag, New York, 2004.

[9] L. C. Evans, *Partial Differential Equations*, American Mathematical Society, Providence, 1998.

[10] G. P. Galdi, *An Introduction to the Mathematical Theory of the Navier-Stokes Equations: Steady-State Problems*, Springer Verlag, New York, 2011.

[11] M. Hanke and M. Brühl, Recent progress in electrical impedance tomography, *Inverse Problems*, **90** (2003), 65–90.

[12] N. Hyvönen, H. Hakula and S. Pursiainen, Numerical implementation of the factorization method within the complete electrode *Inverse Problems and Imaging*, **1** (2007), 299–317.

[13] H. Haddar and G. Migliorati, Numerical analysis of the Factorization Method for EIT with piecewise constant uncertain backgr *Inverse Problems*, **29** (2013), 065009.

[14] H. Heck, G. Uhlmann and J.-N. Wang, Reconstruction of obstacles immersed in an incompressible fluid, *Inverse Problems and Imaging*, **1** (2007), 63–76.

[15] G. C. Hsiao and W. L. Wendland, *Boundary Integral Equations*, Springer Verlag, New York, 2008.

[16] A. Kirsch and N. Grinberg, *The Factorization Method for Inverse Problems*, Oxford University Press, Oxford, 2008.

[17] A. Kirsch, *An Introduction to the Mathematical Theory of Inverse Problems*, Springer Verlag, New York, 2011.
[18] M. Krotkiewski, I. Ligaarden, K.-A. Lie and D. W. Schmid, On the importance of the Stokes-Brinkman equations for computing effective permeability in carbonate karst reservoirs, *Commun. Comput. Phys.*, **10** (2011), 1315–1332.
[19] O. A. Ladyzhenskaya, *The Mathematical Theory of Viscous Incompressible Flow*, Gordon and Breach, London, 1969.
[20] M. Lewicka and S. Müller, The uniform Korn–Poincaré inequality in thin domains, *Annales de l'Institut Henri Poincare - Non Linear Analysis*, **28** (2011), 443–469.
[21] W. C. H. McLean, *Strongly Elliptic Systems and Boundary Integral Equations*, Cambridge University Press, Cambridge, 2000.
[22] C. L. M. H. Navier, Sur les lois du mouvement des fluides, *Mem. Acad. R. Sci. Inst. Fr.*, **6** (1827), 389–440.
[23] P. Popov, Y. Efendiev and G. Qin, Multiscale modeling and simulations of flows in naturally fractured karst reservoirs, *Commun. Comput. Phys.*, **6** (2009), 162–184.
[24] C. Pozrikidis, *Boundary Integral and Singularity Methods for Linearized Viscous Flow*, Cambridge University Press, Cambridge, 1992.
[25] V. Tsiporin, *Charakterisierung Eines Gebiets Durch Spektraldaten eines Dirichletproblems zur Stokesgleichung, (German) [Characterization of a Domain via the Spectral data of a Dirichlet Problem for the Stokes Equation]*, PhD thesis, Georg-August-Universität Göttingen, 2003.
[26] Q. M. Z. Zia and R. Potthast, Flow and shape reconstructions from remote measurements, *Math. Meth. Appl. Sci.*, **36** (2013), 1171–1186.

Received January 2013; 1st revision July 2013; final revision August 2013.

E-mail address: lechleiter@math.uni-bremen.de
E-mail address: rienmueller@uni-bremen.de